Published in final edited form as:
Biomed Microdevices. 2014 April ; 16(2): 311–323. doi:10.1007/s10544-014-9834-8.

A Microfluidic Cell Co-Culture Platform with a Liquid Fluorocarbon Separator

Bryson M. Brewer[1], **Mingjian Shi**[2], **Jon F. Edd**[1], **Donna J. Webb**[2,3], and **Deyu Li**[1,*]

[1]Department of Mechanical Engineering, Vanderbilt University, Nashville, TN 37235-1592

[2]Department of Biological Sciences and Vanderbilt Kennedy Center for Research on Human Development, Vanderbilt University, Nashville TN 37235

[3]Department of Cancer Biology, Vanderbilt University, Nashville TN 37235

Abstract

A microfluidic cell co-culture platform that uses a liquid fluorocarbon oil barrier to separate cells into different culture chambers has been developed. Characterization indicates that the oil barrier could be effective for multiple days, and a maximum pressure difference between the oil barrier and aqueous media in the cell culture chamber could be as large as ∼3.43 kPa before the oil barrier fails. Biological applications have been demonstrated with the separate transfection of two groups of primary hippocampal neurons with two different fluorescent proteins and subsequent observation of synaptic contacts between the neurons. In addition, the quality of the fluidic seal provided by the oil barrier is shown to be greater than that of an alternative solid-PDMS valve barrier design by testing the ability of each device to block low molecular weight CellTracker dyes used to stain cells in the culture chambers.

1. Introduction

Our understanding of cell and molecular biology has vastly improved over the last 100 years; however, the commonly used *in vitro* cell culture/co-culture tools that lead to these advancements are not dissimilar to those used in the early days (Meyvantsson and Beebe 2008). Large dishes and flasks typically used in biological cell culture offer little to no spatiotemporal control over the physical and chemical cues that can affect cell function and behavior (Meyvantsson and Beebe 2008). Thus, the detailed study of cell-cell interactions in culture is somewhat limited. The rapid development of microfluidic cell culture systems provides a solution to overcome these limitations. With the key features of laminar flow, optical transparency, biocompatibility, ease of fabrication, and device features comparable in size to cells, microfluidic cell culture systems are uniquely suited for manipulating the cellular microenvironment, addressing many limitations of traditional cell culture methods and allowing for the in-depth investigation of cellular interactions (Gao et al. 2011; Whitesides 2006; Young and Beebe 2010).

A number of microfluidic cell culture/co-culture platforms have been developed that demonstrate improved control over cell-cell interactions. Designs that use micropatterning of specific molecules on a substrate allow for selective attachment of specific cell types to predetermined regions (Bhatia et al. 1997; Kane et al. 2006; Khetani and Bhatia 2008). Co-flowing laminar streams of fluid have also been used to load and treat cells within particular regions of a microfluidic channel (Lucchetta et al. 2005; Takayama et al. 1999). Alternative

*Electronic mail: deyu.li@vanderbilt.edu

strategies employ the concept of compartmentalization, using microgrooves (Taylor et al. 2005), collagen tracks (Ravula et al. 2007), and semi-permeable membranes (Kimura et al. 2008) to separate cell populations. New cell biology assays have been developed based on the novel capabilities these platforms provide; however, there is still a need for better manipulation and more control of the cellular microenvironment. For example, a successful co-culture device should allow for (1) loading of different cell types into specific compartments, (2) culture of each cell type in its optimal media until reaching confluence, (3) manipulation of one cell population's microenvironment without affecting other nearby populations, and (4) real-time, high resolution imaging (Gao et al. 2011).

The desired functions listed above have been successfully incorporated into a microfluidic cell co-culture device previously reported by the authors. In that design, a pneumatically or hydraulically controlled polydimethylsiloxane (PDMS) barrier is used to separate different cell populations (Gao et al. 2011). Using this approach, cells of different types can be cultured to confluence and transfected or stained individually in cell culture chambers that remain separated by the PDMS valve barrier. Then, upon release of the barrier, different cell populations are allowed to interact in a controlled manner. This platform has been successfully used for various applications, including the observation of dendritic spine and synapse formation among primary hippocampal neurons separately transfected with pre- and post-synaptic markers (Gao et al. 2011; Majumdar et al. 2011) and the investigation of the effects of secreted angiocrine factors on the regulation of tumor growth and migration (Brantley-Sieders et al. 2011). However, despite these positive results, the platform still suffers from some limitations. For example, the valve-enabled PDMS barrier cannot be considered truly reversible because cells, neurites, or other biological material trapped under the PDMS barrier during its actuation would incur physical damage (Hosmane et al. 2011). In addition, the rectangular shape of the region under the PDMS barrier results in a sieve valve effect (Marcus et al. 2006; Melin and Quake 2007) that can permit leakage of some small molecules between the separated cell culture chambers. Although this could be partially remedied by using rounded profiles in the barrier region (Unger et al. 2000), forming a complete seal is still a challenge. In addition, using rounded channels requires more complicated and time-consuming fabrication (Fordyce et al. 2012), making this strategy less than ideal. Thus, in this paper we report an alternative approach to address the issues of barrier reversibility and small molecule leakage without sacrificing the functionality provided by the valve-enabled PDMS barrier platform.

One means of achieving well-sealed, reversible separation of cell populations in microfluidic co-culture platforms is to use a non-solid barrier. Several instances have been demonstrated in the literature for a variety of applications of this strategy. For example, a pinned interface between two immiscible fluids has been achieved by selectively changing the surface chemistry in specific regions of a microchannel (Atencia and Beebe 2005). Using this technique, a stable gas/liquid interface, or virtual wall, can be formed. After channel modification, surface tension will counteract the effects of gravity and confine water to the hydrophilic regions of the microchannel, provided the pressure difference between the air and water phases does not exceed a critical value. This method is particularly useful for applications in which dissolved gas species need to be removed from a liquid, such as extracting dissolved oxygen from water (Hibara et al. 2005). Gas/liquid interfaces may also be employed to expose a gas species to a liquid phase to initiate a chemical reaction or adjust the pH of a solution (Atencia and Beebe 2005). In addition to forming pinned interfaces between gases and liquids, surface modification has been used to stabilize the interface between different immiscible liquids for both vertical (Zhao et al. 2002) and horizontal (Hibara et al. 2002) liquid/liquid interfaces, where surface modification was used to reduce the time of formation and instability of the pinned interface. Pinned interfaces are well-suited for use in drug partitioning studies (Surmeian et al. 2002), ion extraction from

solvents (Maruyama et al. 2004), enzymatic reactions (Maruyama et al. 2003), and formation of membranes through interfacial polymerization (Zhao et al. 2002). However, pinned interfaces created using surface modification present several challenges for biological studies involving cell culture. First, changing the surface chemistry of microchannels requires an additional fabrication step when compared to other microfluidic platforms, complicating device production. Studies have also shown that with decreasing surface wettability via treatment with chemicals such as octadecylsilane, the growth and proliferation of attached cells may be reduced (Altankov et al. 1996). In addition, the critical differential pressure across a pinned liquid/gas or liquid/liquid boundary generated using surface modification may be too low to ensure interface stability in long-term cell culture applications. Thus, difficulties would likely arise in attempting to implement this technique in the construction of a reversible cell culture barrier.

An improved technique incorporates microposts into microfluidic channels to enhance the stability of the interface between two fluids by increasing the critical differential pressure required to rupture the interface (Berthier et al. 2009; Tetala et al. 2009; Xu et al. 2006). One demonstration of this method employs an array of microposts to separate a water-containing middle channel from two outer chambers containing air (Lai et al. 2011). Thus, a virtual wall barrier is formed between two chambers. As long as the critical pressure is not exceeded, water will remain confined to the central channel and not flow into the outer chambers. With careful operation, this method could likely be inverted so that an air layer is used to separate two chambers filled with water. While this type of device was shown to be effective at trapping cells in the regions between microposts (Lai et al. 2011), a few challenges prevent it from being useful for the type of neurobiology and cancer biology studies conducted using the solid-PDMS valve barrier platform. First, in order to create an interface, the PDMS channels were allowed to recover their natural hydrophobic state before loading any water into the device. Hydrophobic channels are less compatible with the more user-friendly passive pumping method (Walker and Beebe 2002) used in our previous studies (Gao et al. 2011). In addition, for channels with sharp corners or other irregular features, a hydrophobic surface increases the chance of small air bubbles forming in the cell culture chamber. Problematically, the presence of air in the cellular microenvironment can be detrimental to cell viability (Skelley and Voldman 2008; Sung and Shuler 2009; Zheng et al. 2010). Reversibility of the valve may also be difficult, particularly when trying to use an air-based virtual wall. Once the channel walls in the valve region are wetted by the aqueous phase, reintroducing a stable air barrier will be very difficult without first completely drying out the entire device. Finally, the permeability of PDMS to air (Hosokawa et al. 2004; Kang et al. 2008; Merkel and Bondar 2000) could result in the degradation of an air-based virtual wall in long-term cell culture by evaporation or condensation. Thus, significant modification of the virtual wall concept is needed for successful implementation into a microfluidic cell co-culture platform.

Here, we present a microfluidic cell co-culture platform that uses a liquid fluorocarbon oil (Fluorinert FC-40) to reversibly separate two cell populations without the need for a surfactant. In this design, two outer cell culture chambers are connected via a series of microgrooves to a middle channel in which FC-40 can be loaded to separate cells from one another without crushing the cell bodies/processes in the barrier region. Liquid fluorocarbons such as FC-40 have been used in a variety of microfluidics applications including droplet actuation (Chatterjee et al. 2006), nanoparticle synthesis (Shestopalov et al. 2004), and cell encapsulation (Köster et al. 2008), and its biocompatibility is well documented (Köster et al. 2008; Lowe et al. 1998; Shi et al. 2010). The FC-40 oil barrier is created by taking advantage of the immiscibility of the fluorocarbon oil (located in the middle channel) and the aqueous media found in the outer cell culture chambers, which can form a stable interface in the reduced cross-sectional area of the connecting microgrooves.

This was achieved without any special surface modifications (other than standard oxygen plasma treatment used for device fabrication) or the necessity of hydrophobic channel walls, and the barrier can remain stable for multiple days. The device was also used to observe the initial synaptic contact between two populations of primary hippocampal neurons separately transfected with different fluorescent proteins. Additionally, results show that the oil separator more effectively blocks the transport of small CellTracker dyes, indicating that it could provide a better fluidic seal than the solid-PDMS valve barrier platform. Finally, it is worth noting that although PDMS was used to fabricate these devices, other materials such as thermoplastics could be used as well, since the operation of the barrier requires no deformation to achieve separation. This is important because PDMS is permeable to many small molecules (Toepke and Beebe 2006) and incompatible with most organic solvents (Lee et al. 2003). Thus, for applications in which these issues are a concern, oil barrier platforms made of alternative materials that do not suffer from permeability problems could be advantageous.

2. Materials and Methods

2.1. Device Fabrication

As shown in Figure 1(a-c), a two-chamber design of the liquid fluorocarbon oil barrier platform consists of two outer cell culture chambers (1 mm × 5 mm × 100 μm; width *(w)*, length (*l*), and height (*h*), respectively) separated by a 200 μm (*w*) × 100 μm (*h*) oil channel. The series of microgrooves connecting the oil channel to the outer culture chambers are each 100 μm (*l*) × 50 μm (*w*) × 5 μm (*h*). The device was fabricated using standard soft lithography techniques (McDonald and Whitesides 2002; Whitesides et al. 2001).

A reusable master mold was created using SU-8 multi-layer photolithography. The 5 μm layer for the connecting microgrooves was patterned by spinning SU-8 2005 (Microchem, Newton, MA) at 2000 RPM for 35 seconds. After pre-baking at 95°C for 2 minutes, the SU-8 was exposed through a photomask (CAD/Art Services Inc., Bandon, OR) with an exposure energy of 390 mJ/cm^2 using a Novacure 2100 Spot Curing System (EXFO Inc., Quebec, CANADA). The 5 μm layer was completed after a 3 minute post-bake at 95°C and development with SU-8 developer (Microchem, Newton, MA). Similarly, the 100 μm layer for the oil channel and cell culture chambers was patterned by spinning SU-8 2050 at 1650 RPM for 35 seconds, pre-baking at 65°C for 5 minutes and 95°C for 20 minutes, manually aligning the photomask with respect to the features of the 5 μm layer and exposing at 390 mJ/cm^2, post-baking at 65°C for 1 minute and 95°C for 10 minutes, and developing for ∼10 minutes with SU-8 developer.

After fabrication of the master, liquid PDMS base polymer was mixed with the curing agent (Ellsworth Adhesives, Germantown, WI) at a 10:1 mass ratio and poured over the mold, which was degassed in a vacuum for ∼1 hour and cured for at least 2 hours at 70°C. After curing, the solid PDMS layer was cut and peeled from the mold, and holes were punched to form the inlets and outlets of each channel. Next, the PDMS device and a glass coverslip (VWR Vista Vision, Suwanee, GA) were treated in a plasma cleaner (Harrick Plasma, Ithaca, NY) and bonded together, forming an irreversible seal. Deionized (DI) water was immediately added to the channels in order to prevent the PDMS from reverting to its natural hydrophobic state (Duffy et al. 1998). Pyrex cloning cylinders (Fisher Scientific, Pittsburgh, PA) were attached to the inlet and outlet reservoirs of the cell chambers using uncured liquid PDMS. In addition, 0.02” I.D./0.06” O.D. Tygon microbore tubing (Cole-Parmer, Vernon Hills, IL) was inserted into the inlet and outlet holes of the middle oil channel and sealed with uncured liquid PDMS. Finally, the assembled device was placed in a 70°C oven for ∼1 hour to cure the PDMS seals around the reservoirs and tubing, during which time the channels remain filled with DI water.

In addition to the two-chamber design, a four-chamber version of the oil barrier device was fabricated using the same protocol, as shown in Figure 1(d-f). The four-chamber version is simply a modified two-chamber design with an outer cell culture chamber and oil channel attached via microgrooves to the right and left of the inner culture chambers. Thus, the four-chamber device contains three oil channels that can be used to independently separate all of the culture chambers. It is worth noting that for the purpose of demonstration, we employed only the central oil channel for all experiments performed in this study. The dimensions of the key features of the four-chamber platform are identical to those of the two-chamber design.

2.2. Static and Dynamic Operation

The FC-40 oil barrier device can function in two schemes: a static approach and a dynamic approach. In the static scheme, the first step is to remove any excess liquid from the inlet and outlet reservoirs of the culture chambers. This helps to achieve a gross pressure balance between the two phases during initial loading. Then, a syringe is used to slowly inject FC-40 into the middle channel, displacing the aqueous phase already there. Once the entire channel and tubing are occupied by the oil, a ¾″ AACO binder clip is used to clamp the tubing, first on the syringe end and then on the open end. This ensures that the oil channel does not become pressurized, causing oil leakage into the outer culture chambers. Media can then be added to the reservoirs as necessary. On the other hand, the dynamic scheme uses a syringe pump (Chemyx Inc., Stafford, TX) to flow oil continuously through the middle channel. A syringe filled with FC-40 is directly attached to the inlet tubing of the middle oil channel; a syringe pump is then used to control the flow rate (up to ∼125 μL/min) to maintain a stable oil barrier. There are advantages for both approaches, depending on the application. The static oil barrier is more user-friendly for biological studies, as the entire device can be contained within a Petri dish, making it easier to maintain a sterile environment as the device is transferred between culture hoods, incubators, and microscopes. However, greater control over the oil/water interface was demonstrated using the dynamic oil barrier, which could be advantageous for applications in which the use of a syringe pump is not problematic. Both strategies were used in this study for characterization of device performance, although only the static oil barrier was used for biological testing.

Proper media flow in the cell culture chambers was achieved using a passive pumping method in which the pressure drop created by a difference in fluid level height between the inlet and outlet reservoirs drives the flow, as we have done previously (Gao et al. 2011). A variety of factors can influence the flow rate in this method, including fluid level, the shape and completeness of the meniscus formed in each reservoir, evaporation, and time since loading media (Lynn and Dandy 2009). Thus, well-determined flow rates were not achieved for this approach; however, as demonstrated previously for similar microfluidic cell culture applications, the passive pumping method is sufficient for supplying cells with fresh media, as well as removing waste from the culture region (Gao et al. 2011). Nonetheless, the Hagen-Poiseuille equation ($\Delta p = R_{hyd} \cdot Q$, where Δp is the pressure drop, R_{hyd} is the hydraulic resistance of a rectangular channel, and Q is the flow rate) can be used to estimate the range of flow rates realized in the device. Using the method, the maximum flow rate just after loading media was estimated to be ∼20-60 nL/s, with the flow rate decreasing over time until the culture media is refreshed.

2.3. Device Characterization

2.3.1. Long-term stability of the static oil barrier—To demonstrate the long-term stability of the FC-40 separator, a static oil barrier was loaded and a water-based fluorescent dye was used to visualize the location of the oil/water interface. Fluorescein isothiocyanate (FITC) (Thermo Scientific, Rockford, IL) was added to one culture chamber after loading

the oil barrier; images were then captured periodically using a Nikon AZ100 fluorescence microscope (Nikon Instruments Inc., Melville, NY). At the end of the experiment, DI water was injected into the middle oil channel, replacing the FC-40. A final image was captured just after (<5 min) removing the oil barrier.

2.3.2. Investigation of the shape of the oil/water interface using confocal microscopy—A more thorough investigation of the oil/water interface was conducted using confocal microscopy. Both a static and dynamic oil barrier with oil flow rates up to 150 μL/min were analyzed. For the static case, an oil barrier was introduced into a device initially filled with FITC. Then, using a Quorum WaveFX spinning disk confocal system equipped with a Nikon Eclipse Ti microscope (Nikon Instruments Inc., Melville, NY) and a Hamamatsu ImageEM-CCD camera with a Plan Fluor 40× objective (N.A. 1.3), a z-stack of images (vertical resolution of 0.2 μm) focused on the oil/water interface at a single microgroove was obtained using MetaMorph imaging software (Molecular Devices, Sunnyvale, CA). Similarly, z-stacks of images were acquired for dynamic oil barriers generated using different flow rates after the oil/water interface had stabilized in the microchannel. These images were post-processed using ImageJ, allowing for visualization of the overhead view and side-view cross-sections, as well as three-dimensional reconstructions of the interface. The radii of curvature of the interface in both planes were determined from these reconstructions to derive the pressure drop across the oil-water interface.

2.4. Cell Culture Protocols

2.4.1. Loading neurons into the two-chamber oil barrier device—Before use in biological study, all microfluidic oil barrier devices were sterilized under UV radiation in a Laminar flow hood for 1-2 hours. After sterilization, the cell culture chambers were coated with 1 mg/mL poly-L-lysine (PLL) (Sigma-Aldrich, St. Louis, MO) in 0.1 M borate buffer (pH 8.5) for 12 hours in an incubator at 37°C. Excess PLL was removed from the chambers by flowing sterilized DI water through the channels for ∼2 hours. The freshly coated chambers were then filled with B27-supplemented Neurobasal™ media (neuronal media) (GIBCO™ Invitrogen, Carlsbad, CA). After waiting 20-30 minutes for equilibration, hippocampal neurons that were isolated from dissected brains of E19 rat embryos (Goslin, K., Asmussen, H., Banker 1998) were loaded into the two inlet reservoirs for the neuronal chambers (50,000 cells per culture chamber) at a density of 5×10^5 cells/mL of neuronal media. Note that no oil was present in the middle channel at this point. The cells were allowed to attach to the PLL coated glass substrate of the cell culture chambers by incubating at 37°C with 5% CO_2 for 3 hours. After attachment, ∼300 μL of B27-supplemented Neurobasal™ media that had been conditioned for 24 hours over a confluent monolayer of glial cells (glia-conditioned media) was added to the inlet reservoirs of each culture chamber; about half of that volume was added to the outlet reservoirs to slow down the flow rate. The glia-conditioned media was replenished every 36 hours, along with the removal of the waste media collected in the outlet reservoirs. A summary of this protocol is shown in Figure 2(a).

2.4.2. Loading glia/neuron co-culture into the four-chamber oil barrier device —The loading of glia/neuron co-culture into the four-chamber device is similar to that with the PDMS valve barrier device (Majumdar et al. 2011, Shi et al. 2013), and the on-chip co-culture of glia helps to increase the transfection efficiency and the stability of synaptic contacts. First, the four-chamber devices were prepared for co-culture by using UV sterilization and coating with PLL as described above. The coated four-chamber devices were then equilibrated using Minimum Essential Medium (MEM) (Invitrogen, Carlsbad, CA) containing 10% horse serum and 0.6% glucose (glia culture media) for 20-30 minutes.

Then, glia that were isolated from 2 day old rat pup brains (Goslin, K., Asmussen, H., Banker 1998) were loaded into the two outermost culture chambers by adding 50 μL of glial cell suspension into the inlet of each chamber (25,000 cells/chamber). The devices were incubated at 37°C for 2 hours to permit cell attachment, after which they were filled with 400 μL of glia culture media and incubated for 4-5 days until confluence was achieved. Note that we did not observe glia spreading into neuronal chamber during this process even though no oil barrier was implemented between the glial chamber and neuronal chamber. After the glia reached confluence in their respective chambers, neurons were loaded into the two inner culture chambers using the above-described procedure. A summary of this protocol is shown in Figure 2(b). To ensure that media flowed from the glial chambers into the neuronal chambers after loading the neurons, 400 μL of fresh neuronal media was added to the glial reservoirs while 200 μL of the same media was added to each neuronal reservoir. This was repeated every 36 hours, along with the removal of waste media.

2.4.3. Separate transfections of hippocampal neurons with GFP and mCherry —After 3-7 days in culture, neurons in each chamber were transfected with GFP and mCherry cDNAs using a modified calcium phosphate method (Zhang et al. 2003). First, a static oil barrier was loaded as described previously. Note that special care was taken to keep the FC-40 oil at 37°C (the temperature of the incubator), as we observed that thermal expansion of the oil as its temperature increased from room temperature (20°C) to 37°C resulted in oil leakage into the cell chambers. To accomplish this, the FC-40, syringe, and syringe tips were heated in the incubator before loading the oil; concurrently, the device was placed on a hot plate just above the incubator temperature (∼39°C) while loading the oil to maintain a stable temperature. After a stable oil barrier was loaded, 50 μL of transfection mixtures containing either GFP or mCherry cDNAs (3-6 μg each) were added to the two inlet reservoirs. A drop of culture media was added to the waste reservoirs after 10-15 minutes to reduce the fluid flow, and the device was placed in a 37°C incubator for 1 hour. The channels were then washed with HEPES-buffered solution (HBS) (pH 7.15) for an additional hour, after which 300 μL of fresh glia-conditioned B27 Neurobasal™ culture media was added to each inlet reservoir. Finally, by releasing the AACO clips and injecting culture media into the inlet tubing of the middle oil channel, the oil barrier was removed by forcing the FC-40 out of the outlet tubing. A summary of this protocol is shown in Figure 2(c).

2.4.4. Confocal microscopy visualization and real-time observation of synaptic contact—The separation of the two culture chambers by the oil barrier was verified by analyzing transfected neurons using confocal microscopy. First, neurons were prepared for live-cell imaging after 12-13 days in culture by replacing neuronal media with 50 mM HEPES containing B27-supplemented Neurobasal™ media without phenol red, pH 7.4. Imaging was performed on the Quorum WaveFX spinning disk confocal system. Cells were imaged using a 10× ADL objective (NA 0.25), a Plan Fluor 40× objective (N.A. 1.3), or a PlanApo 60× TIRF objective (NA 1.49). GFP and mCherry images were obtained by exciting with 491-nm and 561-nm laser lines, respectively (Semrock, Rochester, NY). The resulting images were then analyzed to ensure that no cells were transfected with the inappropriate fluorescent protein.

By transfecting neurons in one chamber with the pre-synaptic marker mCherry-synaptophysin and neurons in the other chamber with GFP, synaptic contact between neurites originating from different culture chambers could be observed. The confocal microscope system was used to obtain two images (one each for mCherry-synaptophysin and GFP) at a given location within a culture chamber. For high magnification images of synapses, a PlanApo 60× TIRF objective (NA 1.49) was used. Images were acquired every 15 minutes for 12 hours using MetaMorph software. The regions along neurites where

synaptic contact occurred were then determined by overlaying the images. In addition, the dynamic formation of synapses over time could be visualized using the time-lapse sequence of overlays. Note that both standard two-chamber oil barrier devices and four-chamber devices with glial co-culture were used to investigate synapse formation between the separately transfected neuronal populations.

2.4.5. Separate staining of hippocampal neurons using CellTracker dyes—To determine the effectiveness of the static oil barrier platform in blocking the transport of smaller molecules between culture chambers, cells in each chamber were stained with CellTracker GreenCMFDA and RedCMTPX (Invitrogen, Eugene, Oregon) fluorescent dyes. As in the transfection protocol, primary hippocampal neurons were cultured for 3-7 days in the microfluidic culture chambers. Then, after loading a stable static oil barrier, 50 μL of fresh glia-conditioned B27 Neurobasal culture media with CellTracker Red (final concentration of 0.5 μM) was added to one inlet reservoir; the same volume of CellTracker Green was added to the other inlet. The device was allowed to incubate at 37°C for ∼1 hour, after which the dyes were flushed using fresh glia-conditioned B27 Neurobasal culture media for 1 hour. This was followed by careful removal of the oil barrier and addition of Neurobasal media containing B27-supplemental without phenol red with 50 mM HEPES, pH 7.4 media. A summary of this protocol is shown in Figure 2(d). As a comparison of device performance, the protocol was repeated with a solid-PDMS valve barrier microfluidic device fabricated using previously detailed procedures (Gao et al. 2011).

3. Results and Discussion

3.1. Barrier Stability

The effectiveness and stability of the FC-40 valve were investigated by loading a static oil barrier and observing how well the barrier confined the fluorescent dye FITC to one culture chamber. As shown in Figure 3, the presence of oil in the middle channel effectively confined FITC to the loading side for ∼72 hours. However, shortly after removing the oil barrier, the FITC was able to quickly migrate into the opposite chamber. Note that the movement of FITC across the oil barrier region and into the opposite cell culture chamber is caused primarily by diffusion, and is likely not the result of a “dragging” effect induced by the water displacing the oil in the middle channel. Significant FITC migration was only observed after the oil was completely displaced and the flow of water in the middle channel stopped. This is consistent with our way of replacing the oil with water through injecting water to push the oil out, rather than withdrawing the oil using negative pressure. These results indicate that the static FC-40 valve is capable of preventing perfusion of small molecules for extended periods of time (>3 days).

It is worth noting that all tests were performed at room temperature (20°C); however, for later biological assays, instabilities in the oil barrier were observed when room temperature FC-40 was added to a device that had been stored in a 37°C incubator. We observed oil leaking into the cell culture chambers shortly after loading the barrier because of thermal expansion of the oil as its temperature increased, which can be determined from the equation

$$\frac{\Delta V}{V_i} = B(\Delta T), \quad (1)$$

where $\Delta V/V_i$ is the relative volume change with respect to the initial volume, is the volumetric coefficient of expansion ($0.0012°C^{-1}$ for FC-40), and ΔT is the change in temperature. According to Eq. (1), an expansion of ∼2% occurs as the oil is heated from 20°C to 37°C. Since the inlet and outlet tubes are clamped, the oil expands into the cell

culture chambers, resulting in the observed leakage. Thus, extra care was needed when conducting biological studies to ensure that both the FC-40 oil and the device were at the same stable temperature. This was achieved by first pre-heating the FC-40 oil and syringe in the 37°C incubator. Then, the entire microfluidic device was placed on a 37-40°C hotplate during the actual loading of the oil barrier. Loading of a static oil barrier typically requires < 5 minutes. By quickly returning the device to the incubator after loading, a stable oil barrier was maintained. For applications in which devices must be removed from the incubator for extended periods of time (i.e. live-cell imaging with the oil barrier loaded), a temperature-controlled microscope stage is recommended, as mismatches in expansion coefficients between the oil and the rest of the device may result in barrier instabilities as the device cools to room temperature. Finally, it is worth noting that the FC-40 is biocompatible and small leakage into the cell culture chamber is fine as long as interference with imaging is not an issue. In fact, we did not observe any detrimental effects on cells that had come into contact with FC-40 that leaked into the culture chambers.

3.2. Interface Characterization

Using confocal microscopy, the interface between the FC-40 and the aqueous phases was examined. The obtained z-stack of images was post-processed to generate both cross-sectional views and three-dimensional reconstructions of the interface. Top and side views of the interface are presented in Figure 4, which shows a single connecting microgroove for both a static and dynamic oil barrier. From these images, a noticeable layer of water (in green) is observed on the sidewalls of the middle channels. This wetting of the channel walls by the aqueous phase is likely a result of the hydrophilic nature of the PDMS after plasma bonding, achieved by keeping the channels immersed in water before testing (Ren et al. 2001). In addition, an ultra-thin boundary layer of water appears to be present at the bottom of the channel on the glass substrate. As expected, the thickness of these aqueous layers decreases as the oil flow rate increases from 0 to 125 μL/min. Although the presence of an ultra-thin residue film of water across the bottom of the oil barrier could potentially result in unwanted mass transport between culture chambers, sensible leakage across the barrier was not observed in any of our biological testing.

As illustrated in Figure 4, the radius of curvature of the oil/water interface in both the overhead and cross-sectional planes decreases with increasing flow rate. By measuring these radii of curvature, the pressure drop across the oil/water interface can be determined using the Young-Laplace equation,

$$\Delta p = \gamma \left(\frac{1}{R_1} + \frac{1}{R_2} \right), \quad (2)$$

in which *Δp* is the pressure drop, is the interfacial tension between water and FC-40 (52.07 mN/m) (Mazutis and Griffiths 2012), and and are the radii of curvature in both planes. The pressure drop values calculated ranged from 0.33 kPa for the static case to 3.43 kPa for the max oil flow rate of 125 μL/min. For an oil flow rate of 150 μL/min, leakage of oil into the cell culture chambers was observed; thus, for an interfacial pressure drop of > ∼4kPa, the surface tension force is overcome by the fluidic pressure in the oil phase, resulting in barrier failure. This analysis also suggests that by decreasing the microgroove dimensions and subsequently, the radii of curvature of the interface, the magnitude of the interfacial pressure drop that can be supported by the device will increase. Note that the pressure drop values calculated here are comparable to or better than those observed in previous virtual wall microfluidic platforms (∼1.5-1.9 kPa) presented in the literature (Lai et al. 2011).

3.3. Separate transfection of hippocampal neurons with fluorescent proteins and observation of synaptic contacts

To demonstrate the usefulness of the FC-40 oil barrier platform for biological applications, primary hippocampal neurons were transfected separately with different fluorescent proteins in each culture chamber, as described in the Methods section. The results of a typical transfection with GFP and mCherry tagged DNAs are shown in Figure 5. Hippocampal neurons in each chamber were transfected with the appropriate fluorescent protein; more importantly, no neurons in the GFP chamber were transfected with mCherry, or vice-versa, indicating that the oil barrier was effective at separating the two chambers. The successful transfection of neurons with GFP and mCherry without any crossover indicates device functionality similar to previous successful microfluidic neurobiology platforms (Gao et al. 2011; Majumdar et al. 2011; Shi et al. 2013).

The successful separate transfection of primary hippocampal neurons with different colored fluorescent proteins allows for dynamic observation of synaptic contact between neurites originating from different culture chambers. In addition, by using the pre-synaptic marker mCherry synaptophysin instead of mCherry in one of the chambers, the location of potential synapses can be easily identified within a culture chamber. In Figure 5(c-e), an area in one of the cell culture chambers near the oil channel is presented that showcases the location of neurites originating from the two culture chambers. By examining the overlay of the images, the locations at which synaptic contact occurs can be readily identified. A sequence of images can also be captured over time, allowing for the observation of the dynamic formation of synapses. This functionality provides the potential to study molecules important to central nervous system synaptic development.

Note that both two-chamber oil barrier devices (using glia conditioned media) and four-chamber devices that contained a co-culture of glia and neurons were successfully used to separately transfect two different neuronal populations and observe synaptic contact. The four-chamber design was employed to increase the transfection efficiency, as improved transfection efficiency using neuron-glia co-culture has been previously demonstrated in the literature (Majumdar et al. 2011). In addition, the four-chamber platform could be useful for applications in which the interactions between several different cell types are to be investigated.

3.4. Separate staining of hippocampal neurons using CellTracker dyes

In addition to transfection with fluorescent proteins, cell staining with commercially available CellTracker dyes was also used to visualize hippocampal neurons in culture. The CellTracker dyes differ from the transfection proteins in that these molecules can penetrate the cell membrane more easily, resulting in staining of nearly 100 percent of the cells in culture. Previously, when staining hippocampal neurons in separate chambers with different colored CellTracker dyes using the solid-PDMS valve barrier device, crossover of the fluorescent molecules was often observed if no special treatment was used to create rounded corners to the microgrooves. As a result, neurons in a chamber that were treated with CellTracker Red exhibited both red and green staining, indicating that the CellTracker Green molecules used in the other culture chamber leaked through the pressurized valve barrier. However, when identical tests were performed using the static oil barrier microfluidic device, no crossover was observed (Figure 6). This result indicates that the oil barrier design could provide a better fluidic seal than the standard solid-PDMS valve barrier platform. Concurrently, no observed leakage of the small CellTracker dye molecules validates the claim that no significant diffusion occurs across the ultra-thin residual aqueous layer that may be trapped below the oil barrier in the middle channel. Thus, the microfluidic oil barrier

platform presented here is an effective option for applications in which small molecules are used to treat separated cell populations.

4. Conclusion

We have developed a microfluidic cell co-culture platform featuring a reversible liquid fluorocarbon (Fluorinert FC-40) barrier that enables separate culture and treatment of cell populations before and/or after allowing the populations to interact with one another. The physical capabilities of the device have been characterized, showcasing that both the stability of the barrier and the maximum pressure drop across the oil/water interface were equal to or greater than that of similar microfluidic platforms reported in the literature. The biological relevance of the device was demonstrated by successful culture and separate transfection of primary hippocampal neurons with different colored fluorescent proteins, allowing for dynamic observation of synaptic contact. The device should be applicable to other co-culture assays that require separate culture and treatment of individual cell populations. More importantly, the liquid fluorocarbon oil barrier design appears to provide a greater fluidic seal between culture chambers, and it exhibits greater biocompatibility than previous solid-barrier based platforms. Even though effective loading/withdrawing of the oil requires some practice, the improved functionality provided by the oil barrier microfluidic cell co-culture platform makes it well-suited for probing cellular and molecular interactions in cell biology studies.

Acknowledgments

B.B. thanks Wan-Hsin Lin and Mingfang Ao for instruction and assistance with the confocal microscope. This work was supported by NIH grants GM092914 (D.J.W.), MH093903 and CA155572 (D.J.W. and D.L.). In addition, this material is based upon work supported by the National Science Foundation Graduate Research Fellowship under Grant No. DGE-0909667. Any opinion, findings, and conclusions or recommendations expressed in this material are those of the author(s) and do not necessarily reflect the views of the National Science Foundation.

References

Altankov G, Grinnell F, Groth T. J Biomed Mater Res. 1996; 30:385. [PubMed: 8698702]

Atencia J, Beebe DJ. Nature. 2005; 437:648. [PubMed: 16193039]

Berthier J, Loe-Mie F, Tran VM, Schoumacker S, Mittler F, Marchand G, Sarrut N. J Colloid Interface Sci. 2009; 338:296. [PubMed: 19596336]

Bhatia SN, Yarmush ML, Toner M. J Biomed Mater Res. 1997; 34:189. [PubMed: 9029299]

Brantley-Sieders DM, Dunaway CM, Rao M, Short S, Hwang Y, Gao Y, Li D, Jiang A, Shyr Y, Wu JY, Chen J. Cancer Res. 2011; 71:976. [PubMed: 21148069]

Chatterjee D, Hetayothin B, Wheeler AR, King DJ, Garrell RL. Lab Chip. 2006; 6:199. [PubMed: 16450028]

Duffy DC, McDonald JC, Schueller OJ, Whitesides GM. Anal Chem. 1998; 70:4974. [PubMed: 21644679]

Fordyce PM, a Diaz-Botia C, Derisi JL, Gomez-Sjoberg R. Lab Chip. 2012; 12:4287. [PubMed: 22930180]

Gao Y, Majumdar D, Jovanovic B, Shaifer C, Lin PC, Zijlstra A, Webb DJ, Li D. Biomed Microdevices. 2011; 13:539. [PubMed: 21424383]

Goslin, G.; Asmussen, K.; Banker, H. Cult Nerve Cells. 2nd. Banker, K.; Goslin, G., editors. MIT Press; Cambridge, MA: 1998. p. 339-370.

Hibara A, Iwayama S, Matsuoka S, Ueno M, Kikutani Y, Tokeshi M, Kitamori T. Anal Chem. 2005; 77:943. [PubMed: 15679365]

Hibara A, Nonaka M, Hisamoto H, Uchiyama K, Kikutani Y, Tokeshi M, Kitamori T. Anal Chem. 2002; 74:1724. [PubMed: 12033266]

Hosmane S, Fournier A, Wright R, Rajbhandari L, Siddique R, Yang IH, Ramesh KT, Venkatesan A, Thakor N. Lab Chip. 2011; 11:3888. [PubMed: 21975691]

Hosokawa K, Sato K, Ichikawa N, Maeda M. Lab Chip. 2004; 4:181. [PubMed: 15159775]

Kane BJ, Zinner MJ, Yarmush ML, Toner M. Anal Chem. 2006; 78:4291. [PubMed: 16808435]

Kang JH, Kim YC, Park JK. Lab Chip. 2008; 8:176. [PubMed: 18094777]

Khetani SR, Bhatia SN. Nat Biotechnol. 2008; 26:120. [PubMed: 18026090]

Kimura H, Yamamoto T, Sakai H, Sakai Y, Fujii T. Lab Chip. 2008; 8:741. [PubMed: 18432344]

Köster S, Angilè FE, Duan H, Agresti JJ, Wintner A, Schmitz C, Rowat AC, a Merten C, Pisignano D, Griffiths AD, a Weitz D. Lab Chip. 2008; 8:1110. [PubMed: 18584086]

Lai HH, Xu W, Allbritton NL. Biomicrofluidics. 2011; 5:24105. [PubMed: 21629561]

Lee JN, Park C, Whitesides GM. Anal Chem. 2003; 75:6544. [PubMed: 14640726]

Lowe KC, Davey MR, Power JB. Trends Biotechnol. 1998; 16:272. [PubMed: 9652139]

Lucchetta EM, Lee JH, a Fu L, Patel NH, Ismagilov RF. Nature. 2005; 434:1134. [PubMed: 15858575]

Lynn NS, Dandy DS. Lab Chip. 2009; 9:3422. [PubMed: 19904410]

Majumdar D, Gao Y, Li D, Webb DJ. J Neurosci Methods. 2011; 196:38. [PubMed: 21185867]

Marcus JS, Anderson WF, Quake SR. Anal Chem. 2006; 78:3084. [PubMed: 16642997]

Maruyama T, Matsushita H, Uchida J, Kubota F, Kamiya N, Goto M. Anal Chem. 2004; 76:4495. [PubMed: 15283593]

Maruyama T, Uchida J, Ohkawa T, Futami T, Katayama K, Nishizawa K, Sotowa K, Kubota F, Kamiya N, Goto M. Lab Chip. 2003; 3:308. [PubMed: 15007464]

Mazutis L, Griffiths AD. Lab Chip. 2012; 12:1800. [PubMed: 22453914]

McDonald JC, Whitesides GM. Acc Chem Res. 2002; 35:491. [PubMed: 12118988]

Melin J, Quake SR. Annu Rev Biophys Biomol Struct. 2007; 36:213. [PubMed: 17269901]

Merkel T, Bondar V. J Polym Sci Part B Polym Phys. 2000; 38:415.

Meyvantsson I, Beebe DJ. Annu Rev Anal Chem (Palo Alto Calif). 2008; 1:423. [PubMed: 20636085]

Ravula SK, Wang MS, a Asress S, Glass JD, Bruno Frazier a. J Neurosci Methods. 2007; 159:78. [PubMed: 16876258]

Ren X, Bachman M, Sims C, Li GP, Allbritton N. J Chromatogr B Biomed Sci Appl. 2001; 762:117. [PubMed: 11678371]

Shestopalov I, Tice JD, Ismagilov RF. Lab Chip. 2004; 4:316. [PubMed: 15269797]

Shi M, Majumdar D, Gao Y, Brewer B, Goodwin C, a McLean J, Li D, Webb DJ. Lab Chip. 2013; 13:3008. [PubMed: 23736663]

Shi W, Wen H, Lu Y, Shi Y, Lin B, Qin J. Lab Chip. 2010; 10:2855. [PubMed: 20882233]

Skelley AM, Voldman J. Lab Chip. 2008; 8:1733. [PubMed: 18813398]

Sung JH, Shuler ML. Biomed Microdevices. 2009; 11:731. [PubMed: 19212816]

Surmeian M, Slyadnev MN, Hisamoto H, Hibara A, Uchiyama K, Kitamori T. Anal Chem. 2002; 74:2014. [PubMed: 12033301]

Takayama S, McDonald JC, Ostuni E, Liang MN, Kenis PJ, Ismagilov RF, Whitesides GM. Proc Natl Acad Sci U S A. 1999; 96:5545. [PubMed: 10318920]

Taylor A, Blurton-Jones M, Rhee S. Nat Methods. 2005; 2:599. [PubMed: 16094385]

Tetala KKR, Swarts JW, Chen B, Janssen AEM, a van Beek T. Lab Chip. 2009; 9:2085. [PubMed: 19568679]

Toepke MW, Beebe DJ. Lab Chip. 2006; 6:1484. [PubMed: 17203151]

Unger MA, Chou HP, Thorsen T, Scherer A, Quake SR. Science (80-). 2000; 288:113.

Walker GM, Beebe DJ. Lab Chip. 2002; 2:57. [PubMed: 15100834]

Whitesides GM. Nature. 2006; 442:368. [PubMed: 16871203]

Whitesides GM, Ostuni E, Takayama S, Jiang X, Ingber DE. Annu Rev Biomed Eng. 2001; 3:335. [PubMed: 11447067]

Xu W, Xue H, Bachman M, Li GP. Conf Proc IEEE Eng Med Biol Soc. 2006; 1:2840. [PubMed: 17946533]

Young EWK, Beebe DJ. Chem Soc Rev. 2010; 39:1036. [PubMed: 20179823]
Zhang H, Webb DJ, Asmussen H, Horwitz AF. J Cell Biol. 2003; 161:131. [PubMed: 12695502]
Zhao B, Viernes NOL, Moore JS, Beebe DJ. J Am Chem Soc. 2002; 124:5284. [PubMed: 11996566]
Zheng W, Wang Z, Zhang W, Jiang X. Lab Chip. 2010; 10:2906. [PubMed: 20844778]

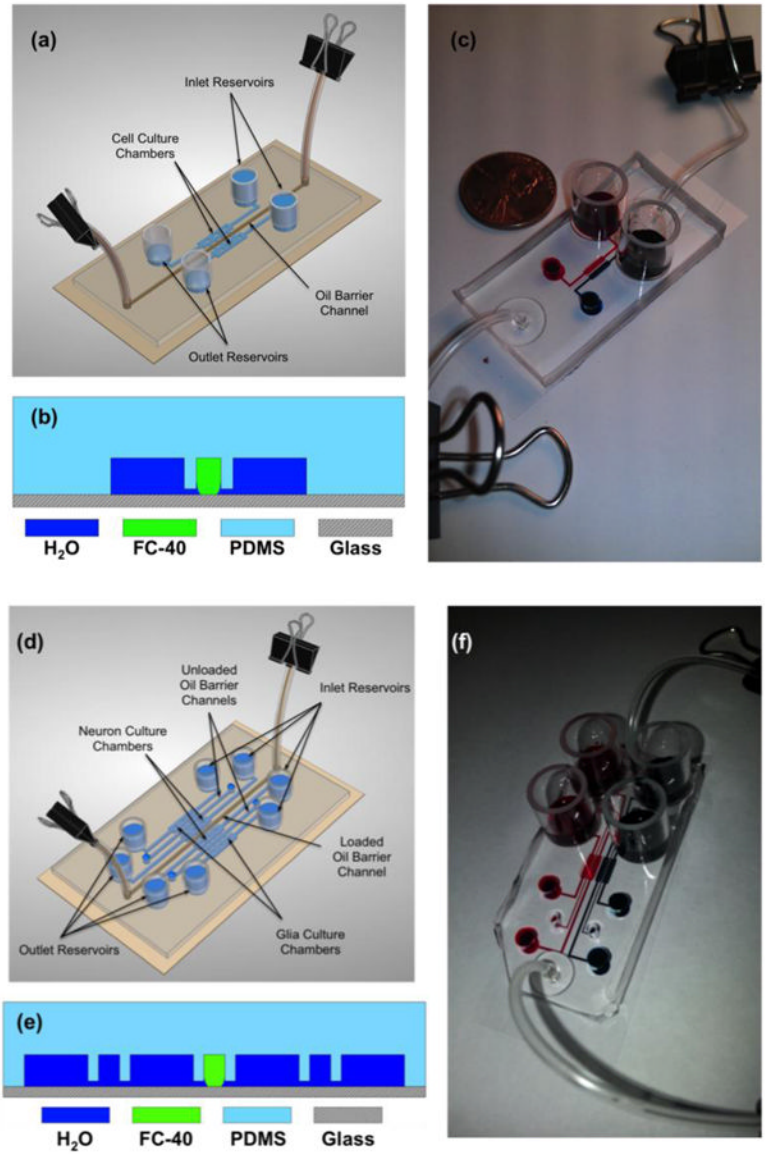

Figure 1. Design of the fluorocarbon oil barrier microfluidic platform

(**a**) Three-dimensional cartoon of a loaded, static oil barrier device. (**b**) A cross-section diagram of the device showing the fluidic connection between the outer cell culture chambers and the middle oil channel via microgrooves (not to scale). (**c**) A photograph demonstrating a static oil barrier device separating red dye in the left culture chamber from blue dye in the right culture chamber. A U.S. penny is shown for scale. (**d**) Three-dimensional cartoon of a static four-chamber oil barrier device in which the middle oil channel is loaded with FC-40. Note that for the experiments performed in this paper, only the center oil channel was filled with oil. However, all chambers may be isolated from one another by filling all three oil channels with FC-40. (**e**) A cross-section diagram of the four-chamber device, showcasing the fluidic connection between the glia in the outer chambers and the neurons in the inner chambers. (**f**) A photograph demonstrating a static oil barrier isolating the two chambers with red dye on the left from the two chambers with blue dye on the right.

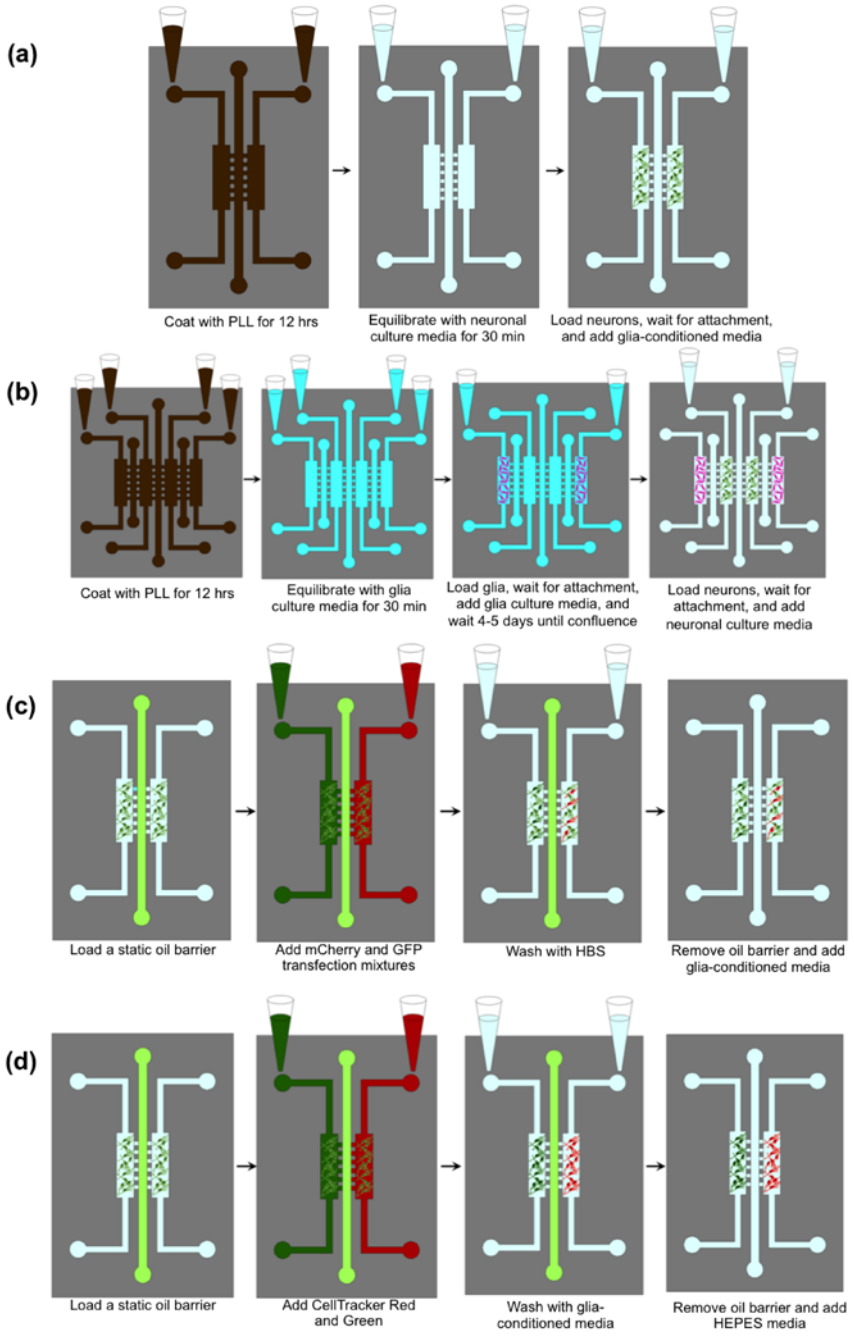

Figure 2. Summary of the biological cell-culture protocols using the oil barrier platform

(**a**) Loading neurons in the two-chamber oil barrier device. (**b**) Loading glia, then neurons into the four-chamber oil-barrier platform. (**c**) Transfecting neurons with mCherry and GFP (same procedure used in four-chamber devices). (**d**) Staining neurons with CellTracker Red and Green (same procedure used in four-chamber devices).

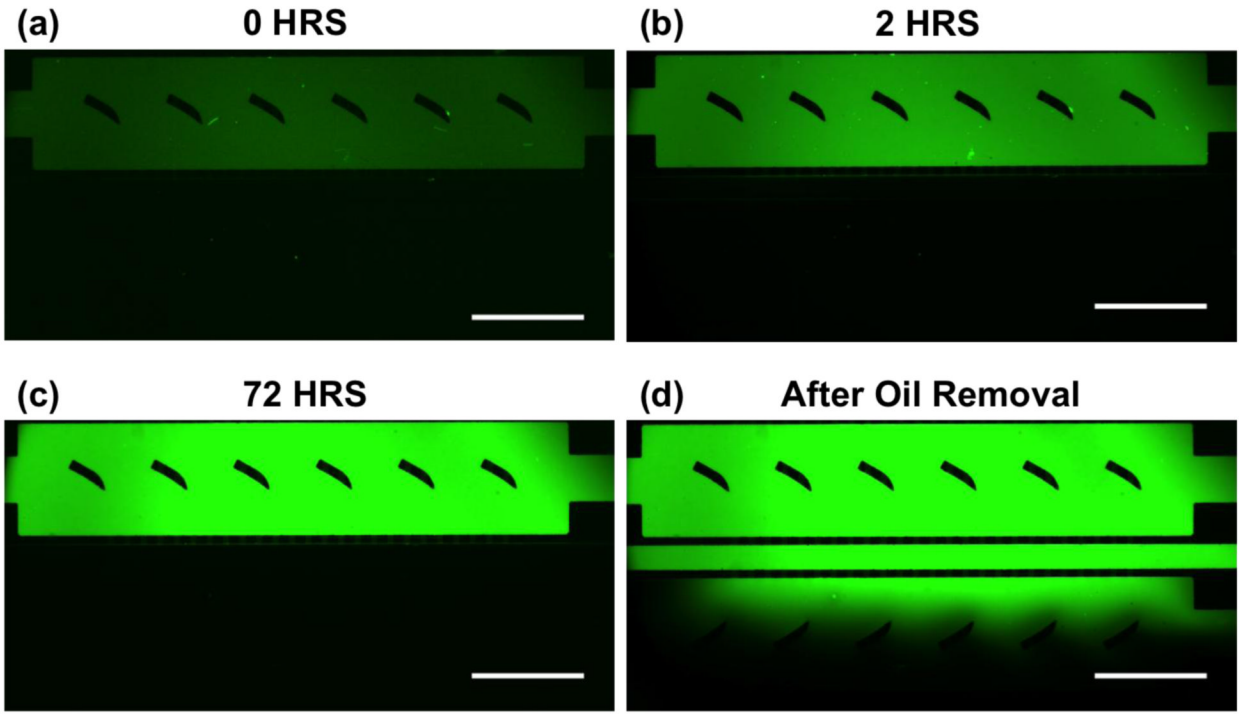

Figure 3. Demonstration of the long-term stability of a static oil barrier device using FITC

Fluorescent images were obtained (**a**) immediately after loading the static oil barrier, (**b**) after 2 hours, (**c**) after 72 hours, and (**d**) after removing the oil barrier (< 5 minutes). Note that the concentration of FITC in the device increases over time due primarily to evaporation of the aqueous solvent. The scale bar is 1 mm.

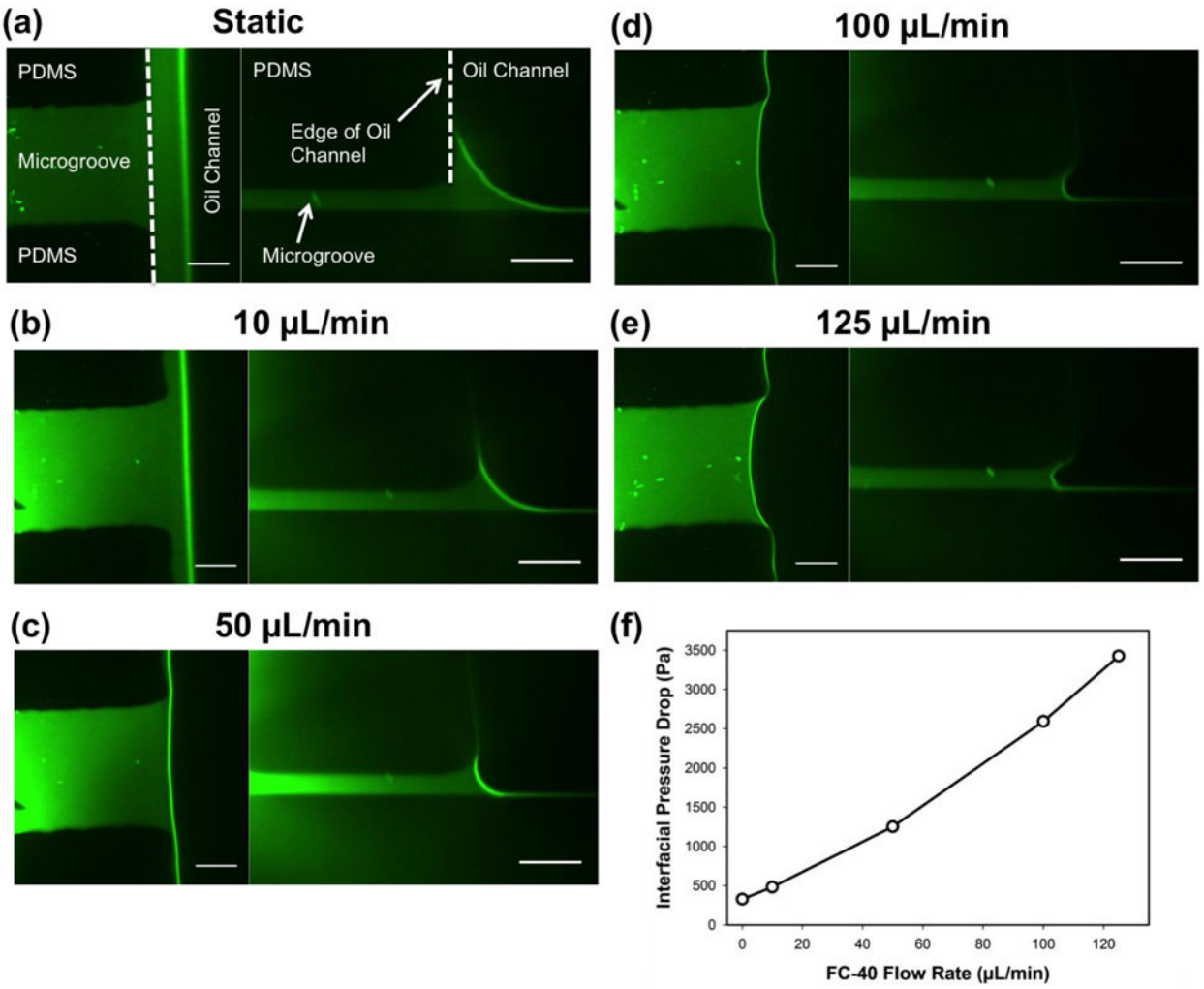

Figure 4. Top-view images and cross-sectional reconstructions of the oil/water interface in both static and dynamic oil barrier devices

FITC was used to visualize the aqueous phase. (**a**-**e**) The oil flow rate was increased from 0 μL/min to 125 μL/min for each z-stack of images captured. (**f**) The interfacial pressure drop between the higher pressure oil phase and lower pressure aqueous phase as a function of FC-40 flow rate as calculated using the Young-Laplace equation. The scale bar in all images is 20 μm.

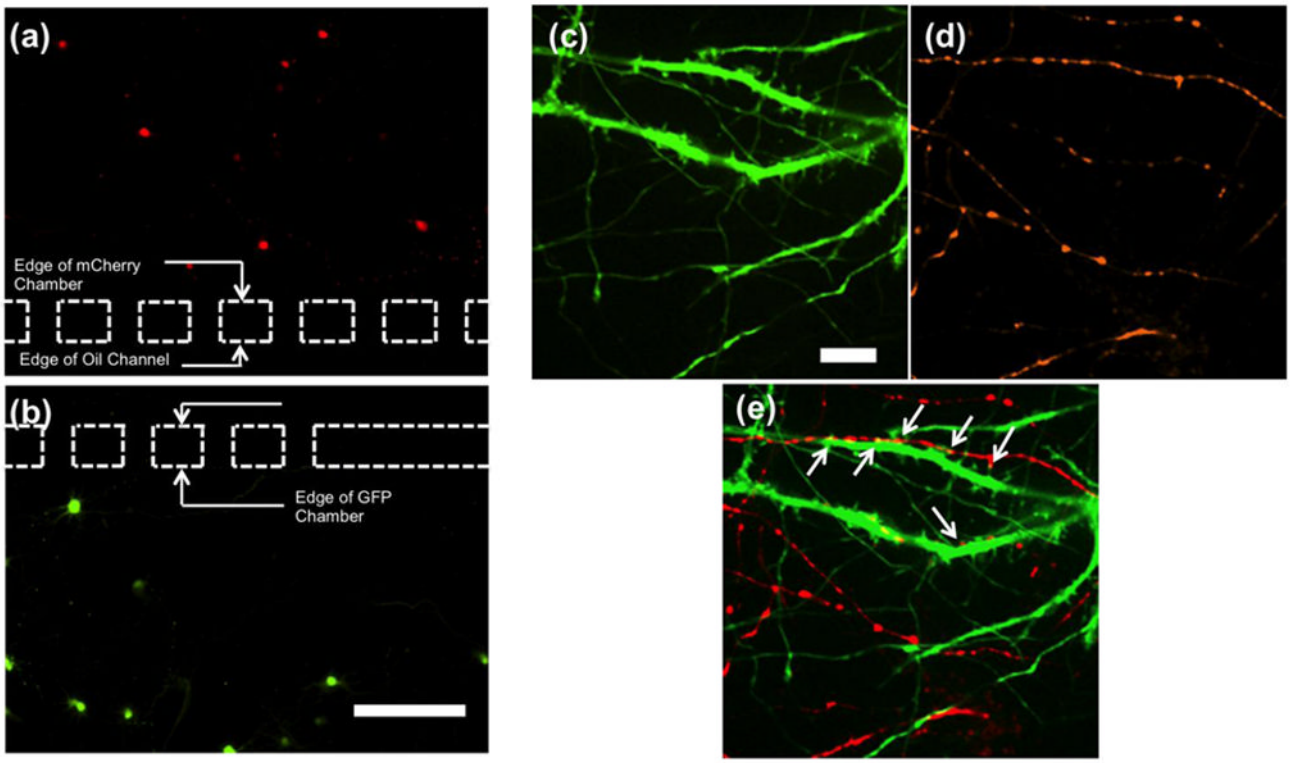

Figure 5. Separate transfection of primary hippocampal neurons with fluorescent proteins using the static oil barrier platform and the subsequent dynamic observation of synaptic contact

(**a-b**) Neurons were transfected with mCherry in the top panel and GFP in the bottom panel. The dashed lines illustrate the location of the microgrooves connecting the respective chambers to the oil channel. Note that no neurons in the mCherry chamber were transfected with GFP, or vice-versa. The scale bar is 200 μm. (**c-e**) Two images using different fluorescent filters were obtained at the same location in one of the cell culture chambers (near the oil barrier region), demonstrating contact between neurons from the adjacent chambers. Neurons in one chamber were transfected with (**c**) GFP, while neurons in the other chamber were transfected with (**d**) mCherry synaptophysin. (**e**) An overlay of the two images allows the locations of synaptic contacts to be identified. The areas indicated by the white arrows are observed synaptic junctions. The scale bar is 10 μm.

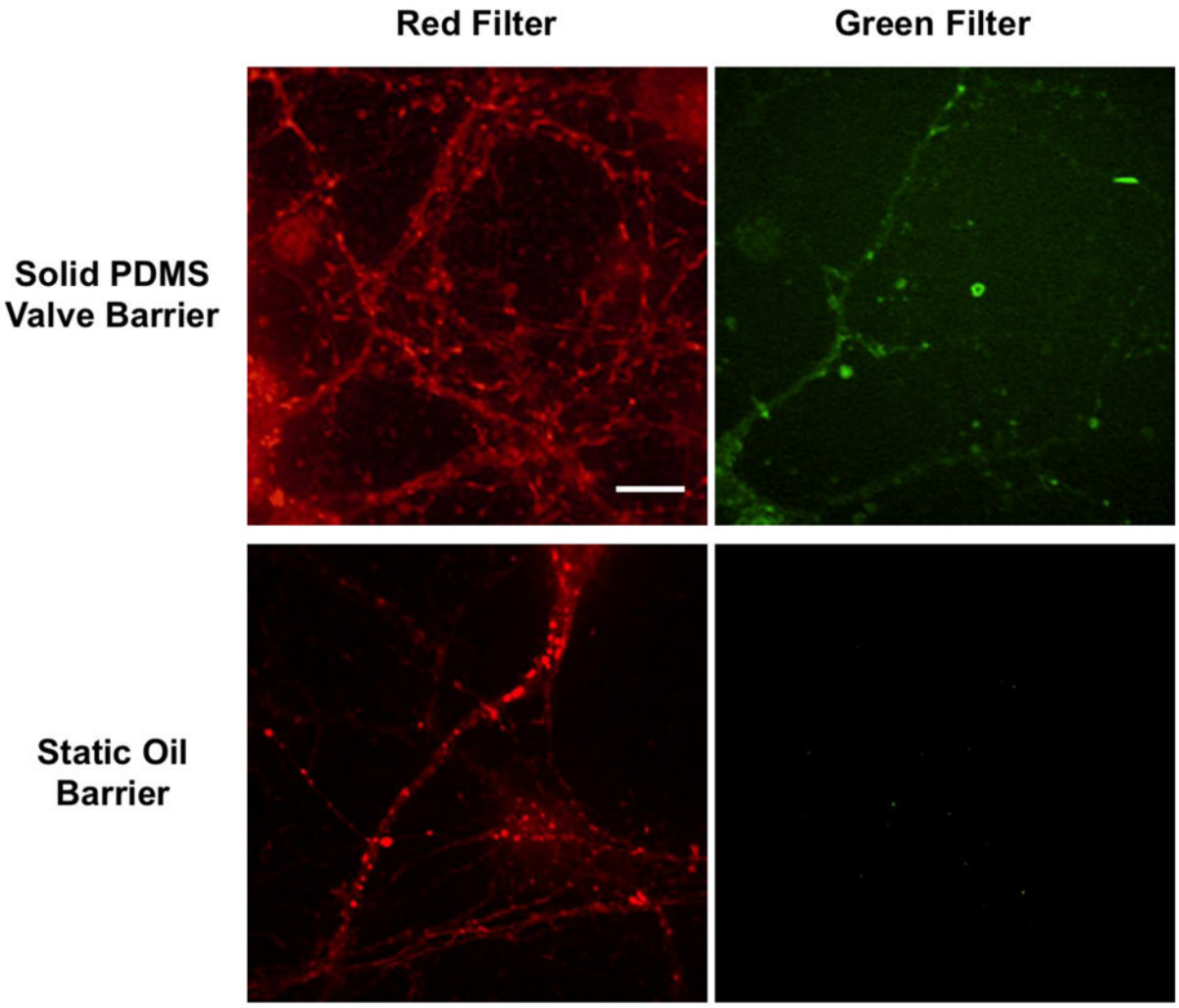

Figure 6. Using CellTracker Red and Green to compare leakage of the solid-PDMS valve barrier microfluidic platform to the static oil barrier device

For each device, neurons in one culture chamber were stained with CellTracker Red, while neurons in the opposite chamber were stained with CellTracker Green. In the top panels, confocal images were obtained at the same location in the culture chamber treated with CellTracker Red using both red and green filters. The results indicate that cell structure was stained with both CellTracker Red and Green, suggesting leakage of CellTracker Green across the solid-PDMS valve barrier. However, in the bottom panels, images taken in the chamber treated with CellTracker Red show cell structure stained red only; thus, the oil barrier appears to more effectively block the transport of small CellTracker molecules between culture chambers. The scale bar is 10 μm.